Pure & Appl. Chem., Vol. 66, No. 6, pp. 1381-1388, 1994.
Printed in Great Britain.
© 1994 IUPAC

Real-time monitoring of surface chemistry during plasma processing

E. S. Aydil*, R. A. Gottscho†, and Y. J. Chabal†

*University of California Santa Barbara, Department of Chemical and Nuclear Engineering, Santa Barbara, California 93106, USA
†AT&T Bell Laboratories, 600 Mountain Av., Murray Hill, NJ 07974, USA

Abstract: Techniques available for real time, *in situ* monitoring of surface chemistry during plasma processing are reviewed. Emphasis is given to recent uses of attenuated-total-reflection Fourier transform infrared (ATR-FTIR) spectroscopy to study surface bond vibrations during plasma cleaning and passivation of Si and GaAs surfaces. Examples are chosen to demonstrate the utility of real-time monitoring of surfaces for developing and optimizing plasma processes used in manufacturing of electronic and optoelectronic devices.

INTRODUCTION

Surface reactions and kinetics are among the least understood phenomena in plasma processing of materials (1). Surface reactions pertaining to plasma-assisted etching, deposition and cleaning are often studied, under well-controlled ultra high vacuum (UHV) conditions, using surface analysis techniques such as X-ray photoelectron spectroscopy (XPS), Auger electron spectroscopy (AES), etc. Most of these techniques require UHV and can not be used in higher pressure plasma environments. While UHV surface analysis provides a wealth of information on surface chemistry, in many cases, it is unclear how this information can be used under plasma environments to develop new processes and optimize existing ones. Unfortunately, diagnostic techniques that can be used to obtain direct information on surface chemistry *in situ* and in real time are scarce. In this paper, some of the techniques available to study surfaces *in situ* and in real time during plasma processing are reviewed. Examples are chosen from plasma processing of electronic materials for integrated circuit manufacturing. Emphasis will be given to the recent uses of attenuated-total-reflection Fourier transform infrared spectroscopy (2-7) to study surface bond vibrations during plasma cleaning and passivation of Si and GaAs surfaces (6-7).

ATTENUATED TOTAL REFLECTION FOURIER TRANSFORM INFRARED SPECTROSCOPY (ATR-FTIR)

Attenuated-total-reflection Fourier transform infrared spectroscopy is one of the possible arrangements for performing surface infrared spectroscopy and is particularly well suited for studying surface adsorbates on non-absorbing substrates with relatively high index of refraction, n_s, such as semiconductors (2). ATR-FTIR spectroscopy has been used as a surface diagnostic for the last two decades (2-4), however its use under plasma processing conditions, *in situ* and in real time, is only recent (5-7). In ATR-FTIR spectroscopy, infrared output from a FTIR spectrometer is focused at normal incidence onto one of the beveled faces of a GaAs (or Si) crystal and traverses the sample undergoing multiple internal reflections as shown in Fig. 1. If the angle of incidence onto the substrate-vacuum interface is larger than the critical angle, $\theta_c=\sin^{-1}(1/n_s)$, the transmitted field is evanescent and the radiation is totally internally reflected. In this manner, a large electric field is created at the vacuum side of the substrate-vacuum interface which can then interact with surface dipoles and excite surface species (2).

Experimental (2,6,7)

The samples used in ATR-FTIR experiments are cut from semiconductor wafers (≈0.05-0.07 cm thick) into rectangular pieces typically 5-10 cm long by a few cm wide with 45° bevels at each of the short

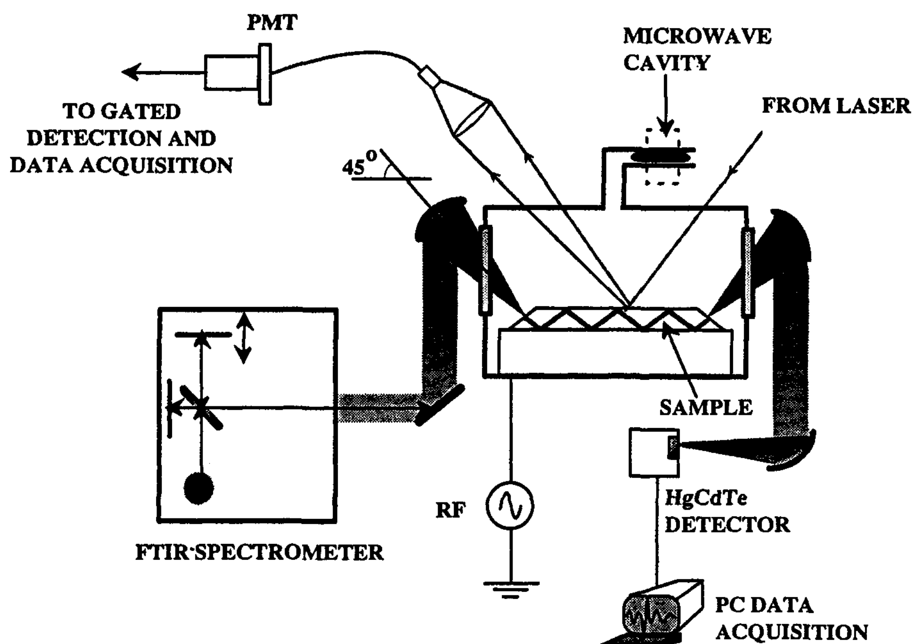

Fig. 1 Schematic of an ATR-FTIR setup (Ref. 6).

sides. In a typical experimental arrangement, such as the one shown in Fig. 1, infrared radiation from the external port of an FTIR spectrometer is directed and focused onto one of the beveled edges, entering the chamber through an infrared transparent window (*e.g.*, KBr). The IR radiation enters the input bevel at normal incidence with some angular spread ($\approx \pm 5$-$10°$) and hits the bottom surface at 45° (greater than θ_c). Thus, infrared radiation is trapped in the sample and traverses its length, exiting from the opposite beveled edge. After leaving the chamber through another window, the transmitted beam is collected and focused onto a detector (*e.g.*, HgCdTe) by either reflective or refractive optics. The number of reflections, N, from the top surface is given by L/2d where L is the sample length and d is the thickness: typically N ≈ 10-100. The IR optical path outside the chamber is enclosed and purged with dry, CO_2-free N_2 to eliminate gas phase absorption by H_2O and CO_2 present in the ambient. This also prevents fogging of IR- transparent windows and lenses (*e.g.*, KBr) which are often hygroscopic.

In situ Investigation of Plasma-Assisted Si Surface Cleaning with ATR-FTIR (7)

Silicon surface cleaning is a critical process in semiconductor manufacturing. In particular, there has been recent interest in developing dry cleaning methods using gaseous reagents in lieu of wet techniques (*e.g.*, HF etching). ATR-FTIR spectroscopy has been used to study and optimize room temperature, H-atom based plasma (H_2 and NH_3) cleaning of native oxide and carbon contaminated Si surfaces (7). As an example, Fig. 2 shows the spectrum obtained from a HF-cleaned sample overlaid with that of a H_2 plasma treated sample. Both ATR-FTIR spectra were taken in the so-called differential mode where the spectrum of a plasma (or HF) cleaned sample is divided by the spectrum of an untreated sample. An increase in transmission is observed at the absorption frequency of the chemical bonds that were present on the surface prior to cleaning but are removed by the plasma treatment. Similarly, a decrease in transmission is observed at the absorption frequency of the chemical bonds that are formed as a result of the plasma exposure. From the spectra in Fig. 2, one can conclude that while O-H bonds are removed and Si-H bonds are formed in both treatments, hydrocarbons are removed only with the plasma process. Judging from the IR spectra, H_2 plasma treatment is as effective as HF cleaning. Assignment of the spectral features is discussed in Ref. 7 in detail. Assignments made in spectra obtained in a plasma environment generally draw upon assignments made in studies conducted under well-defined UHV conditions with several surface analysis techniques. Fortunately, the literature concerned with surface infrared spectroscopy studies, particularly on semiconductor surfaces, is growing (2). Wherever possible isotopic substitution is used to check the assignments.

Real-Time Monitoring of Species Surface Densities

Time evolution of the species concentration on the surface can be determined using ATR-FTIR by monitoring the frequency-integrated intensity of the vibrational bands. Ignoring coverage dependent effects, the surface concentration in monolayers, ρ, is proportional to the area under the absorption feature and can be estimated from

$$\int \frac{\Delta I}{I_o} d\tilde{v} = \int (1 - T(\tilde{v}))\, d\tilde{v} \approx N\rho \int A(\tilde{v})\, d\tilde{v} \approx \alpha N \rho \quad , \tag{1}$$

for T<<1, where T is the transmittance, α is the frequency integrated absorption coefficient, and N=L/2d is the number of passes. In order to evaluate α (6,7), we draw upon the UHV studies where coverages are measured with two independent techniques one of which is ATR-FTIR. The absolute concentrations obtained in this manner are estimated to be within a factor of two or three. However the accuracy of the relative concentrations is only limited by signal to noise ratio and generally better than 10%. The time resolution depends on the spectral resolution and, typically, spectra can be collected <1 s. However, sometimes a compromise must be made between temporal resolution and signal to noise ratio since averaging of several spectra may be necessary.

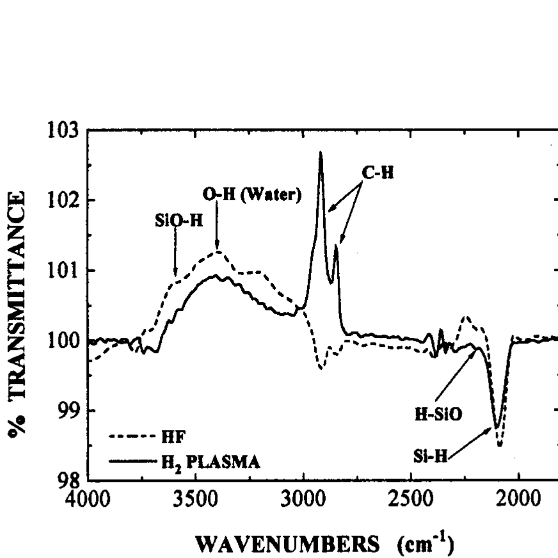

Fig. 2 ATR-FTIR spectrum of a H_2 plasma cleaned Si surface compared with the spectrum of a HF cleaned surface (Ref. 7).

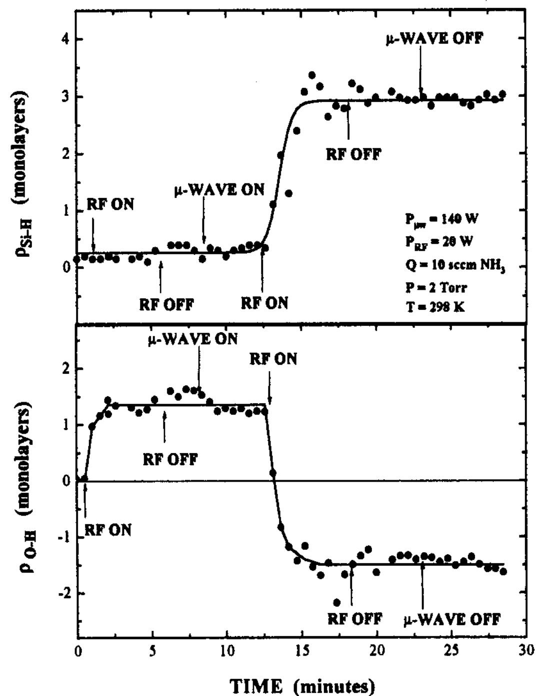

Fig. 3 Real time variations in (a) Si-H and (b) O-H stretching absorptions as microwave and rf powers are sequentially turned on and off.

To illustrate the power of real-time monitoring, the density of the Si-H and O-H bonds in monolayers (ML) is shown in Fig. 3 as a function of time as the plasma exposure conditions are changed. In this experiment, a hybrid plasma processing reactor was used to clean Si surfaces (7): the hybrid process utilized a combination of an upstream microwave plasma and separate rf biasing of the sample platen to control the ion bombardment. When the microwave plasma is turned on without the rf bias, the sample is exposed to H atoms alone and is not bombarded by ions. On the other hand, when the rf bias is turned on, a plasma is visible over the sample which is then bombarded by both ions and H atoms: the ratio of ion energy flux to H flux, R, to the sample surface can be manipulated by varying the ratio of the

microwave power to the rf power, pressure, and flow rate. Figure 3a shows the surface Si-H density as the plasma excitation method is changed from pure rf (high R) to pure microwave (R=0) to a combination of the two. During the first 5 minutes, the sample is exposed to an rf plasma through NH_3 at 2 Torr, 10 sccm and 20 W rf for 20 minutes. No Si-H is observed but a broad absorption at 3400 cm^{-1}, attributed to O-H stretching of physically adsorbed H_2O, appears on the native oxide contaminated Si surface(8). The surface density of O-H is plotted in Fig. 3b. Next, the rf is turned off and the microwave plasma is turned on at 140 W, while maintaining all other plasma parameters constant, but still no Si-H is observed. These results show that neither ion flux without a high H atom flux nor a high H atom flux without ion bombardment is effective in removing the native oxide and passivating the Si surface by forming Si-H bonds. However, an interesting result is observed when the rf power is turned on while the microwave plasma is still on: Si-H absorption increases rapidly while the O-H absorption decreases rapidly. Combined action of the ion bombardment created by the rf plasma and H atom flux from the upstream microwave plasma remove water, hydroxides, hydrocarbons and oxygen to leave behind a H terminated hydrophobic surface (7).

Evolution of the surface concentration of various species during the treatment gave tremendous insight into optimizing the cleaning process. For example, it was found that having too low of a H-atom flux to ion bombardment energy ratio resulted in incomplete removal of the native oxide and formation of H-SiO on the surface which could be detected easily since it causes Si-H absorption to shift to higher frequencies. The plasma parameters suitable for cleaning Si surface were found by adjusting the flow rate and rf power (thus manipulating the H flux to ion energy flux ratio) and monitoring the region of the spectrum where Si-H absorbs. As an example, Fig. 4 shows the ATR-FTIR spectra obtained when Si is treated with a hybrid (140 W microwave power, 1 Torr) plasma for 2 minutes using either 10 W rf power and 10 sccm H_2 flow (dashed spectrum) or 3 W rf power and 50 sccm H_2 flow (solid spectrum). Absorption by Si-H and OSi-H is evident in the dashed spectrum which was too rich in ion energy flux relative to the neutral H atom flux. The solid curve corresponds to a process where H atom flux to the surface was increased by increasing the flow rate and ion energy flux was reduced by decreasing the rf bias. In the latter case, H-SiO is removed completely and the surface is left passivated with approximately 1-2 monolayers of H.

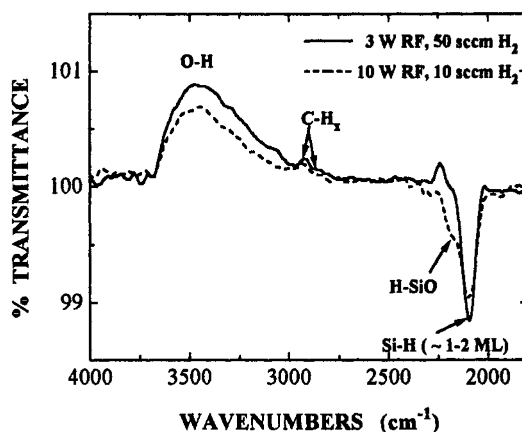

Fig. 4 Si ATR-FTIR spectra relative to an untreated sample. The dashed curve corresponds to a process that was too rich in ion flux relative to H flux. The solid curve corresponds to an optimized process (Ref. 7).

INFRARED REFLECTION ABSORPTION SPECTROSCOPY (IRRAS)

Like ATR-FTIR, IRRAS is a surface infrared spectroscopy technique better suited for studying surface adsorbates and optically thin films (film thickness<<wavelength) on absorbing substrates such as metals (2). In this technique, p-polarized infrared radiation from a source is directed onto the substrate surface at grazing incidence, typically at 80-85° with a small angular spread. The experimental and optical arrangement is otherwise similar to ATR-FTIR spectroscopy apparatus. The incident p-polarized radiation creates a high electric field on the vacuum side of the substrate-vacuum interface (or in the optically thin film at that interface) which can then interact with and excite surface species (or bonds in the film). IRRAS is a well-established technique in UHV surface experiments to study strong absorbers, like CO, on metal surfaces (2,9,10). Recently, IRRAS has been applied to real-time detection of Si-H bonds incorporated into amorphous silicon films as they grow on metal surfaces by plasma-assisted deposition (11). Unfortunately, it is well known that IRRAS is not a sensitive technique for studying adsorbates on semiconductors because they are dielectrics in the mid-IR region of the spectrum (2, 12). To increase the sensitivity of IRRAS for studying adsorbates or films on semiconductors, burried metal layer IRRAS (BML-IRRAS) technique has been proposed and demonstrated by Bermudez (12-15). In

BML-IRRAS, an optically thin but physically thick semiconductor layer is deposited on a metal substrate to form a surface with physical properties of a semiconductor and optical properties of a metal. In UHV studies the technique has been demonstrated for O_2, H_2O and H_2 on GaAs (12) and CF_3 on Si (15). IRRAS has also been used *in situ* and in real time by Leu and Jensen (16) to monitor $NF_3/CF_4/O_2$ microwave downstream plasma etching of polyimide and poly(methyl-methacrylate).

PHOTOLUMINESCENCE

Luminescence from semiconductor surfaces are sensitive to surface states in the band gap and can be sensitive to adsorbates on the surface (17-23). In photoluminescence diagnostic technique, the substrate is excited by photons with energies larger than that of the band gap. Electron-hole pairs are created by absorption of this energy which can subsequently recombine and emit near-bandgap radiation. A typical arrangment for PL measurements is shown schematically in Fig. 1 along with the ATR-FTIR set up. A pulsed or a chopped continuous-wave laser beam is focused onto the surface and PL is collected at right angles to the laser propagation direction. Gated detection or lock-in techniques are used to discriminate against the plasma background emission. Collected PL can be analyzed at a particular wavelength or a spectrum can be collected using a monochromator. Although experimentally simple, interpretation of PL data is difficult because the PL yield can be affected by a number of phenomena. Thus, the technique is most effective when used with a complimentary surface diagnostic technique such as ATR-FTIR or when the nature of the PL change is known.

H-Atom Based Plasma Passivation of GaAs Surfaces (6, 19-20)

Poor electronic properties of GaAs surfaces and GaAs-insulator interfaces resulting from a high density of surface/interface states limit GaAs device technology. H-atom based plasma passivation techniques using H_2, NH_3,and H_2S, have emerged as viable methods for removing native oxides and surface states thought to be caused by excess elemental As at oxide-insulator interfaces (24). To illustrate the use of PL in conjunction with ATR-FTIR, we briefly discuss an example where passivation of GaAs surfaces with a downstream microwave NH_3 plasma is investigated: ATR-FTIR and PL measurements have been shown to be tremendously valuable tools for optimizing the process conditions.

Experiments are performed in the same apparatus used for Si cleaning but without rf biasing the sample platen. Using ATR-FTIR, the relative concentrations of -As-O, -As-H, -H_2O, and -CH_x bonds are measured as a function of exposure to the effluent from a microwave discharge through NH_3 and H_2. The PL intensity from the GaAs surface is monitored simultaneously and used qualitatively to estimate the extent of surface state (due to As antisite defect, As_{Ga}) reduction. When the density of surface states due to the As_{Ga} is high, PL intensity is reduced due to nonradiative recombination. When the surface states are reduced PL yield is increased.

Figures 5a-c display the integrated intensity of the -As-O, -O-H (from physically adsorbed H_2O) and As-H respectively. PL intensity is superimposed on these figures. Figures 5a-c show that -As-O bonds disappear while -O-H and -As-H bonds appear after the plasma is gated on at t=1 minute. The initial increase in O-H concentration coincides with disappearance of -As-O bonds suggesting that H_2O is formed on the surface by reduction of the As-O bonds. The long term slow rise in surface water concentration is attributed to water formed by reaction of H with the quartz reactor walls and transported to the surface via diffusion and flow where it physically adsorbs on the surface [6]. The enhancement in PL intensity is significantly delayed from plasma initiation and removal of As-O bonds. Interestingly, the formation of -As-H bonds is also delayed by an equal amount and follows the same functional dependence as the As-H bonds. Since the source of the mid-gap states, elemental As, is at the oxide-GaAs interface, it seems reasonable that the rates of As-H formation and PL enhancement may be limited, at least partly, by diffusion of H through the oxide and the water layer. The presence of As-H bonds after the treatment indicates that some As-H may be trapped at this interface.

Figure 6 shows how PL monitoring can be used in real time to optimize the exposure time during rf parallel-plate NH_3 plasma treatment of GaAs surfaces. In the parallel plate reactor, the plasma is directly over the sample surface which is bombarded and damaged with energetic ions. Figure 6b shows that PL intensity drops abruptly after the first few seconds of direct exposure and an initial increase. This decrease in PL is attributed to surface damage by ion bombardment which introduces surface states and thus degrades the PL yield. The damaging action of ion bombardment and passivating action of H atoms counteract to produce a maximum in the PL vs. time curve. The PL intensity in this

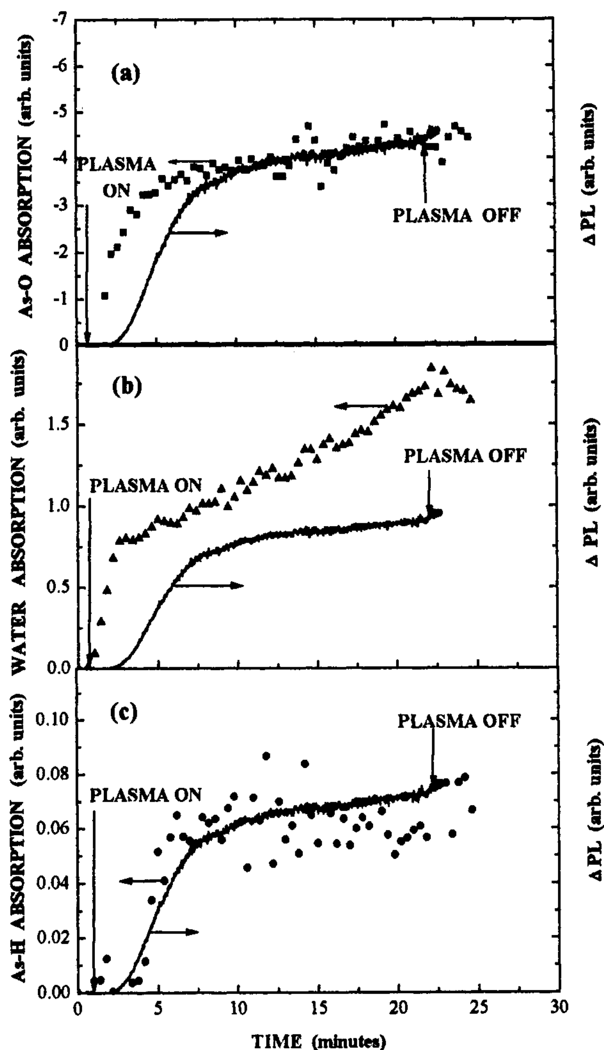

Fig. 5 Real time changes in (a) As-O, (b) H-OH and (c) As-H absorption during NH_3 plasma passivation of GaAs. Photoluminescence intensity is superimposed on each figure. Plasma is turned on at t=1 minute and turned off at t=22 minutes. Pressure, microwave power and flow rate are maintained at 2 Torr, 140 W and 10 sccm respectively

case is very sensitive to the exposure time and only a few seconds separates a successful passivation from damaged surface with a low PL yield. Figure 6a shows how PL monitoring can be used to stop the treatment at the maximum, before the decline in PL starts, avoiding unnecessary ion bombardment damage.

ELLIPSOMETRY

Ellipsometry is one of the more common surface diagnostic techniques used for *in situ* real time monitoring during plasma processing. In this technique, the substrate surface is illuminated by light with a known polarization and the change in polarization upon reflection is measured. For example, when linearly polarized light is reflected off the substrate surface, the reflected beam is elliptically polarized and the ellipticity provides information about optical properties of the films or adsorbates on the substrate. Specifically, complex reflectance ratio,

$$\tilde{\rho} = \frac{r_p}{r_s} = \tan\Psi\, e^{i\Delta}, \qquad (2)$$

is measured in terms of the ellipsometric angles Δ and Ψ where r_p and r_s are the reflection coefficients for p-polarized and s-polarized radiation respectively. The principles of ellipsometry is reviewed in reference 25. The ellipsometric angles are measured experimentally and depend on the optical properties of the substrate and its overlayers. The optical properties in turn can be related to the nature of the overlayers and ellipsometry can thus provide indirect information on surface chemistry. For example, ellipsometry has been used to characterize the fluorosilyl reaction layer formed during etching of Si with F containing plasmas (CF_4, SF_6) (26,27). Oehrlein examined the thickness of this surface layer as a function of plasma conditions and in real time and concluded that Si etching proceeds by formation of a damaged Si layer which is subsequently fluorinated and consumed (26). Silicon surface damage (28) and Si surface roughening (29,30) during plasma etching are among the investigations conducted using ellipsometry.

The complex reflectance ratio, $\tilde{\rho}$, can be measured using a monochromatic or a polychromatic light source. In the the latter case, spectroscopic ellipsometry, $\tilde{\rho}$ is obtained as a function of wavelength. Using spectroscopic ellipsometry, Hu *et al.* studied, *in situ*, the effect of hydrogen ion bombardment of Si and electron cyclotron resonance Si oxidation (31,32). *In situ* ellipsometry has been used in the UV, visible and infrared regions of the spectrum (33). Blayo and Drevillon studied the growth of hydrogenated amorphous silicon by *in situ* infrared ellipsometry (34,35). Of course, ellipsometers can also be used to measure film thicknesses during etching or deposition, in real time, within ≈1 Å (36,37). In fact, ellipsometry is used for this purpose on fabrication lines for real-time process control (36,37). Use of ellipsometers for *in situ* real time surface diagnostic is more common than, for example, infrared absorption spectroscopy. Limited space prevents us from reviewing even a fraction of the ellipsometry literature. Ellipsometry is a powerful technique which can provide insight into the phenomena occurring on surfaces during plasma processing, especially if it is used with a complimentary technique such as ATR-FTIR which can provide direct information on the surface chemistry.

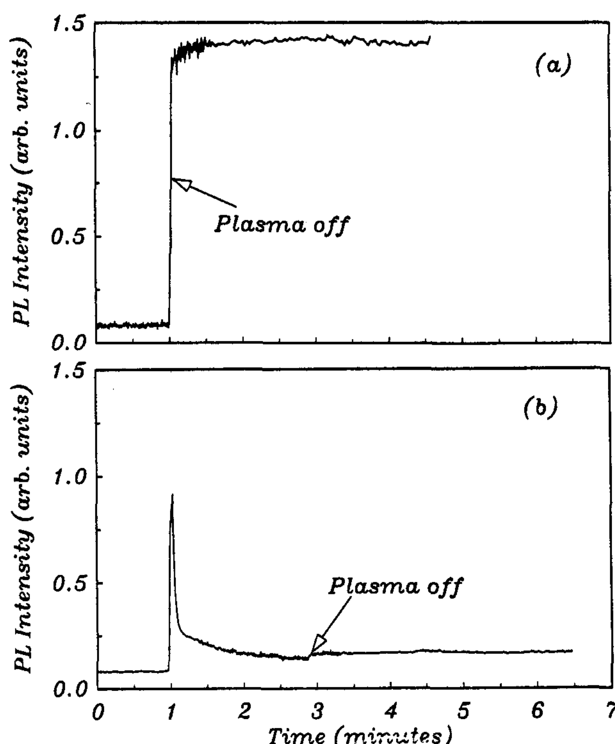

Fig. 6 The effect of exposure time on the PL intensity: (a) 2 seconds, and (b) 2 minutes. A NH_3 rf-parallel-plate plasma at 4 Torr, 20 W power was used (Ref. 20).

SUMMARY

In situ, real-time surface diagnostic techniques are invaluable for probing heterogeneous kinetics during plasma processing. Mechanistic insight into the surface reactions can be gained from such diagnostic techniques which in turn can be used to develop or optimize plasma-assisted etching, deposition and cleaning processes. Surface infrared spectroscopy has been in the arsenal of UHV surface analysis techniques and, recently, been shown to be a promising technique for obtaining information on chemical nature of surfaces during plasma processing.

ACKNOWLEDGEMENTS

We thank V. M. Donnelly, K. P. Giapis, J. A. Gregus, M. Vernon, E. Yoon, and Z. Zhou who have contributed to the work reviewed here. We thank S. Deshmukh for a critical reading of the manuscript.

REFERENCES

1. J. Proud, R. A. Gottscho, J. Bondur, A. Garscadden, J. V. Heberlein, G. K. Herb, M. J. Kushner, J. E. Lawler, M. A. Lieberman, T. M. Mayer, A. V. Phelps, W. Roman, H. Sawin, H. F. Winters, J. Perepezko, A. U. Hazi, C. F. Kennel, and J. Gerardo, *Plasma Processing of Materials: Scientific Opportunities and Technological Challenges*, National Research Council, Panel on Plasma Processing of Materials, National Academy Press, Washington D. C., pp 41-43, pp 57-61 (1991).
2. Y. J. Chabal, *Surf. Sci. Repts.* **8**, 211 (1988).
3. Y. J. Chabal, in *Internal Reflection Spectroscopy: Theory and Applications*, edited by F. M. Mirabella, Jr., Marcel Dekker, New York, (1992).
4. Y. J. Chabal, E. E. Chaban, S. B. Christman, *J. Electron. Spectrosc. Related Phenomena*, **29**, 35 (1983).
5. K. Kawamura, S. Ishizuka, H. Sakaue, and Y. Horiike, *Jpn. J. Appl. Phys.* **30**, 3215 (1991).
6. E. S. Aydil, Z. H. Zhou, K. P. Giapis, Y. J. Chabal, J. A. Gregus, and R. A. Gottscho, *Appl. Phys. Lett.* **62**, 3156 (1993); E. S. Aydil, Z. H. Zhou, R. A. Gottscho, and Y. J. Chabal, *J. Vac. Sci. Technol.* submitted (1993).
7. Z. H. Zhou, E. S. Aydil, R. A. Gottscho, Y. J. Chabal, and R. Reif, *J. Electrochem. Soc.*, in press (1993).
8. Y. J. Chabal and S. B. Christman, *Phys. Rev. B* **29**, 6974 (1984).
9. M. A. Chesters. *J. Mol. Struct.* **173**, 405 (1988).
10. W. Erley, *J. Electron Spectrosc. Rel. Phen.* **44**, 65 (1987).
11. Y. Toyoshima, K. Arai, A. Matsuda, and K. Tanaka, *Appl. Phys. Lett.* **57**, 1028 (1990).
12. V. M. Bermudez and S. M. Prokes, *Surf. Sci.* **248**, 201 (1991).
13. V. M. Bermudez, *J. Vac. Sci. Technol.* **A 10**, 152 (1992).
14. V. M. Bermudez, *J. Vac. Sci. Technol.* **A 10**, 3478 (1992).
15. V. M. Bermudez, *Appl. Phys. Lett.* **62**, 3297 (1993).
16. J. Leu and K. F. Jensen, *J. Vac. Sci. Technol.* **A 9**, 2948 (1991).
17. K. Mettler, *Appl. Phys.* **12**, 75 (1977).
18. R. R. Chang, R. Iyer, and D. L. Lile, *J. Appl. Phys.*, **61**, 1995 (1987).
19. R. A. Gottscho, B. L. Preppernau, S. J. Pearton, A. B. Emerson, and K. P. Giapis, *J. Appl. Phys.* **68**, 440 (1990).
20. E. S. Aydil, K. P. Giapis, R. A. Gottscho, V. M. Donnelly, and E. Yoon, *J. Vac. Sci. Technol.* **B 11**, 195 (1993).
21. H. Idriss, R. M. Andrews, and M. A. Barteau, *J. Vac. Sci. Technol.* **A 11**, 209 (1993).
22. H. Nagai, Y. Noguchi, *Appl. Phys. Lett.* **33**, 312 (1978).
23. E. Yoon, R. A. Gottscho, V. M. Donnelly, and W. S. Hobson, *J. Vac. Sci. Technol.* **B 10**, 2197 (1992).
24. F. Capasso and G. F. Williams, *J. Electrochem. Soc.* **129**, 821 (1982).
25. R. M. Azzam and N, M, Bashara, *Ellipsometry and Polarized Light*, North Holland Amsterdam (1977); R. M. Azzam, editor, *Selected Papers on Ellipsometry*, SPIE Optical Engineering Press, Bellingham, Washington (1991).
26. G. Oehrlein, *J. Vac. Sci. Technol.* **A 11**, 34 (1993).
27. M. A. Jaso and G. S. Oehrlein, *J. Vac. Sci. Technol.* **A 6**, 1397 (1988).
28. M. Haverlag, D. Vender, and G. S. Oehrlein, *Appl. Phys. Lett.* **61**, 2875 (1992).
29. D. J. Thomas, P. Southworth, M. C. Flowers, and R. Greef, *J. Vac. Sci. Technol.* **B 8**, 516 (1990).
30. D. J. Thomas, P. Southworth, M. C. Flowers, and R. Greef, *J. Vac. Sci. Technol.* **B 7**, 1325 (1989).
31. Y. Z. Hu, M. Li, K. Conrad, J. W. Andrews, E. A. Irene, M. Denker, M. Ray, and G. McGuire, *J. Vac. Sci. Technol.* **B 10**, 1111 (1992).
32. Y. Z. Hu, J. Joseph and E. A. Irene, *Appl. Phys. Lett.* **59**, 1353 (1991).
33. B. Drevillon, *Thin Solid Films* **183**, 157 (1988).
34. N. Blayo and B. Drevillon, *Appl. Phys. Lett.* **59**, 950 (1991).
35. B. Drevillon and R. Benferhat, *J. Appl. Phys.* **63**, 5088 (1988).
36. S. A. Henck, *J. Vac. Sci. Technol.* **A 10**, 934 (1992).
37. H. G. Tompkins, B. Vasquez, T. Mathis, and G. Yetter, *J. Electrochem. Soc.* **139**, 1772 (1992).